Cask Assembly Level Modeling to Determine Used Nuclear Fuel Assembly Loading Environments Resulting From Normal Conditions of Rail Transport – 14511

John Bignell *, Gregg Flores *, Douglas Ammerman *
* Sandia National Laboratories

Sandia National Laboratories is a multi-program laboratory managed and operated by Sandia Corporation, a wholly owned subsidiary of Lockheed Martin Corporation, for the U.S. Department of Energy's National Nuclear Security Administration under contract DE-AC04-94AL85000.

ABSTRACT

Sandia National Laboratories (SNL), as part of a larger collaborative effort between SNL, Pacific Northwest National Laboratory (PNNL), Idaho National Laboratory (INL), Oak Ridge National Laboratory (ORNL), and the Transportation Technology Center Inc. (TTCI) focused on assessing the performance of a typical UNF assembly subject to loads stemming from normal conditions of transport (NCT) by rail, has performed cask assembly level modeling and analyses. The intent of these analyses was two-fold. First, to determine the loading environments generated at each fuel assembly by rail car excitations for use in subsequent detailed fuel assembly analyses; and second to assess the sensitivities of those response characteristics to a limited set of model parameters. A series of explicit non-linear transient dynamic analyses were performed using the commercially available finite element code LS-DYNA. The rail cask model employed was of generic design and consisted of a cask body, cask lid, neutron shield, impact limiters, canister body, canister lid, basket support structure, 32-cell fuel basket, and fuel assemblies. Materials were modeled as elastic, but interface gaps between the various components were explicitly included in the model to capture nonlinearities in the response generated by slip and contact between components. Several cask assembly model configurations were investigated with each model configuration being subjected to several load cases comprised of ten second acceleration time-history extracts from longer measured (coal car) or simulation-generated (NUCARS®) rail car acceleration time-history datasets provided by TTCI. Results from the analyses indicate that shock loads were significant enough in some instances to produce slip and/or vertical separation between the fuel assemblies and basket, and impact of the fuel assemblies against the basket cell walls or the top or bottom spacer blocks. This was particularly true for the shock load cases derived from the measured coal car accelerations, and to a lesser extent for the load cases derived from the NUCARS® simulations (which are more representative of the conditions that would be expected for UNF transported by rail). The severity of the loads with respect to the performance of the fuel rods was not readily assessable from the cask level response data; however, the generation of loads sufficient to cause sliding, loss of contact, and impact between components is not desirable. Vibration loads, while somewhat more benign, did produce significant excitations in the frequency range of fuel assembly response. Sensitivity analyses performed indicate that the loading environments generated at each basket cell are relatively insensitive to cask component temperature, modestly sensitive to the inclusion or exclusion of control assembly components with each fuel assembly, and particularly sensitive to cell location and component-to-component clearance sizes.

INTRODUCTION

With nuclear power generation remaining a significant portion of the United States' energy production portfolio the inventories of used nuclear fuel (UNF) continue to grow. At the end of 2012 it was estimated that the commercial nuclear reactor fleet had generated approximately 70,000 metric tons of uranium (MTU) contained in about 245,000 UNF assemblies. By 2020, that number is expected to reach 88,000 MTU [1]. The implementation of any consolidated storage plan for UNF, including those of the Blue Ribbon Commission on America's Nuclear Future [2] and DOE's Strategy for the Management and Disposal of Used Nuclear Fuel and High-Level Radioactive Waste [3], will necessitate transportation of large amounts of UNF. It is desirable that UNF rods maintain their integrity during handling, transportation, and storage to ensure maintenance of the fuel retaining boundary, safety against criticality, and long term fuel retrievability for processing and disposal. Consequently, understanding the mechanical performance of UNF rods under cumulative loading stemming from handling, normal conditions of transport (NCT), and normal conditions of storage (NCS) is important to successfully achieving that end.

The U.S. Department of Energy (DOE) Office of Nuclear Energy, Office of Fuel Cycle Technology has established the Used Fuel Disposition Campaign (UFDC) research effort to investigate technical issues related to storage, transportation, and disposal of UNF and high-level radioactive waste. An important part of the UFDC's research effort is the investigation of the performance of UNF assemblies and components subject to mechanical loads stemming from NCT and NCS. As part the UFDC, a collaborative research effort was undertaken in 2013 involving Sandia National Laboratories (SNL), Pacific Northwest National Laboratory (PNNL), Idaho National Laboratory (INL), Oak Ridge National Laboratory (ORNL), and the Transportation Technology Center Inc. (TTCI) that focused on assessing the performance of a typical UNF assembly subject to loads stemming from normal conditions of transport (NCT) by rail. As part of this collaboration SNL performed cask assembly level modeling. The intent of the cask assembly analyses was two-fold. First, to determine the general characteristics of the shock and vibration environments generated at the fuel assemblies due to rail car excitations associated with NCT for use in subsequent detailed fuel assembly modeling and fuel pin failure assessments; and second to assess the sensitivities of those response characteristics to a limited set of previously identified parameters such as basket cell location, cask assembly component temperature, component-to-component gap size, and the inclusion or exclusion of fuel assembly control components. What follows is an overview of the cask assembly model utilized to perform these analyses, a description of the development of the load cases used to represent the normal conditions of rail transport, and a summary of the analyses performed and conclusions drawn from those analyses.

CASK MODEL DESCRIPTION

The cask model consists of several major components, namely the cask, canister, fuel basket, and fuel assemblies. It was intended to be generic in design, with basic dimensions loosely based on the GBC-32 definition provided in [4]. Inputs to the model included material property and temperature distribution data provided in [5] and [6], rail car excitation data from TTCI [6, 7], and model inputs from PNNL defining the parameters of the simplified sub-models used to represent the fuel assemblies in the cask model. The total mass of the cask in the cask assembly FEM was approximately 123,000 kg (270,000 lbm) exclusive of the approximately 13,600 kg (30,000 lbm) cradle. Interface gaps between the cask and canister, the canister and basket, and the basket and surrogate fuel assemblies were each explicitly included in the model. The possibility of nonlinearities in the response of the cask components to rail car excitations (particularly with respect to contact between components) necessitated that explicit nonlinear analyses be performed. The general purpose finite element program LS-DYNA [8, 9] was utilized for the analyses.

The cask and cradle portion of the cask assembly model was comprised of the cask body, neutron shield, impact limiters, and cask cradle (Figure 1). The cask body consisted of a 200 mm thick open hollow cylinder 5.3675 m long and 2.185 m in outer diameter. Four securement and handling trunnions were located mid-height on each side of the cask body 4.510 m apart (center-to-center) with the outer interface surface located 1.275 m radially out from the cask body central axis. The cask lid and cask body bottom plate were both 300 mm thick. The cask body and lid material were type 304 stainless steel. Surrounding the cask body along 4.760 m of its length was a 132.5 mm thick neutron shield. The neutron shield was made from an NS-4-FR like material. The impact limiters attached to each end of the cask body were 1.250 m long and 3.250 m in outer diameter. Each impact limiter overlapped the cask body by 300 mm. The impact limiters were made from a crushable aluminum honeycomb material. The total assembled length of the cask was 7.2675 m, width was 3.250 m, and height including cradle was 3.400 m. Contact interactions between the cradle elements and the cask body were not included in the simulation because the cradle elements did not represent a true geometric recreation of a cradle structure, but rather simply acted to transfer the rail car excitations to the four trunnions on the cask body. (This is why the cradle elements appear to pass through the body of the cask in Figure 1.)

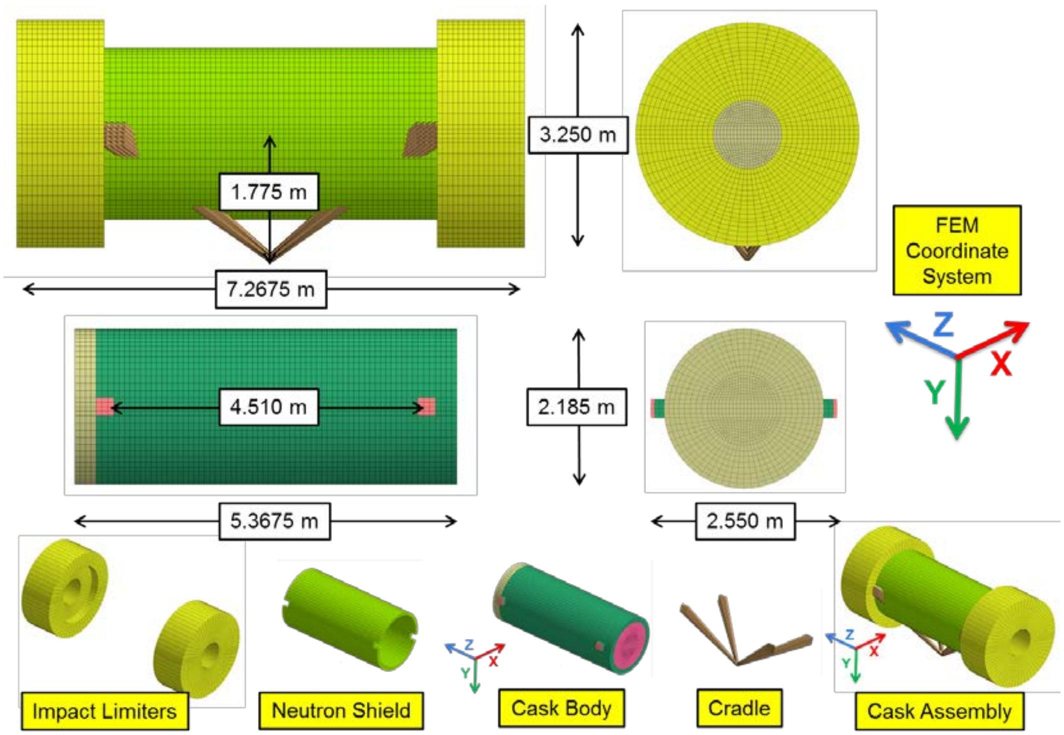

Figure 1: Cask Components of Cask Assembly Model.

The canister and basket portion of the cask assembly model were comprised of the canister body, canister lid, and basket (Figure 2). The canister body consisted of a 12.5 mm thick open hollow cylinder 4.750 m long and 1.775 m in outer diameter. The canister lid and canister bottom plate were 150 mm and 50 mm thick, respectively. Running longitudinally along the inner wall of the canister were four separate structures that provide lateral and vertical support to the basket during cask transport. These support structures consisted of 7.5 mm thick plate elements that run the full length of the basket. The canister component materials were all type 304 stainless steel. The basket consisted of 32 open-ended square cells constructed from 7.5 mm thick plate material. These basket plates were also of type 304 stainless steel. Attached to each cell wall, with the exception of the cell walls on the exterior surface of the basket, were Boral (boron carbide and aluminum) neutron poison plates that run the full length of the basket. The mass and geometric dimensions (for contact) of the Boral plates were included in the model, but they were assumed to contribute no structural stiffness to the basket cell walls.

The fuel assembly and spacer block portion of the cask assembly model was comprised of 32 individual fuel assemblies and 64 top and bottom spacer blocks (Figure 2 and Figure 3). Two fuel assembly configurations were investigated. The first configuration included a representation of the control rod assembly components. This fuel assembly was 4.228 m in length and had a maximum width and height of 214.2 mm (set by the spacer grid dimensions). The second configuration did not include the control rod assembly components. It had a total length of 4.058 m and identical width and height dimensions as the fuel assembly with control components. The various portions of the fuel assembly model (e.g., tie plates, spacer grids, fuel rods, etc.) were represented with either an isotropic or orthotropic elastic material model with parameters selected for those models so as to match the dynamic response characteristics of the simplified model to that of PNNL's detailed-fuel-assembly model.

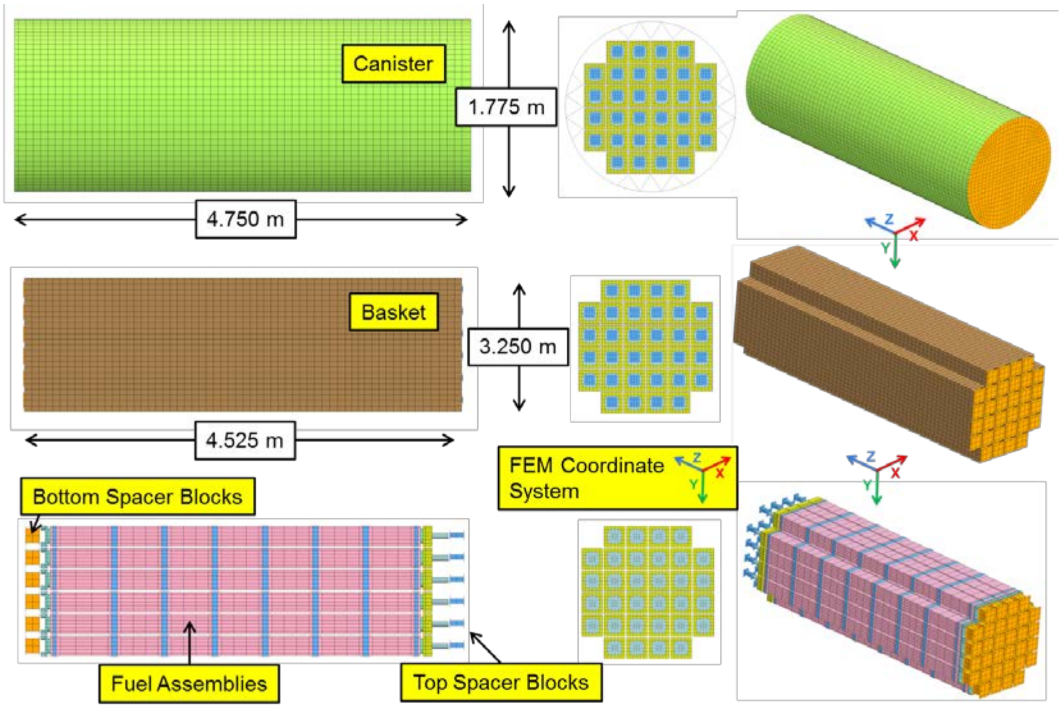

Figure 2: Canister, Basket, and Fuel Assembly Components of Cask Assembly Model.

Both types of fuel assembly were significantly shorter than the interior length of the canister which necessitated that spacer blocks be used to limit the amount of axial movement of the fuel assemblies in the basket during transport. Two types of spacer blocks were employed. The first type, the bottom spacer block, was composed of a 160 mm x 160 mm square type 304 stainless steel tube with a wall thickness of 10 mm, capped on each end with 10 mm thick square plates with dimensions of 210 mm by 210 mm. The bottom spacer block had a total length of 154.58 mm in the case of the fuel assembly with control components, and 239.74 mm for the fuel assembly without control components. Each bottom spacer block was free floating within the fuel basket, but because of the relatively small clearances between each spacer block and its surrounding cell walls its overall movement was limited. The second type of spacer block was the top spacer block which was composed of a 70 mm by 70 mm square type 304 stainless steel tube with a wall thickness of 10 mm, capped on each end with 10 mm thick square plates with dimensions of 120 mm by 120 mm. The top spacer block has a total length of 154.58 mm in the case of the fuel assembly with control components, and 307.55 mm for the fuel assembly without control components. In the case of the fuel assembly without control components, the top spacer block extended into a cavity that existed on the upper tie plate so as to maintain a gap between the spacer block and fuel assembly that was consistent with the fuel assembly with control components case. Unlike the bottom spacer block, the top spacer block was not free floating, but rather was attached to the lid of the canister. The bottom and top spacer block materials were type 304 stainless steel.

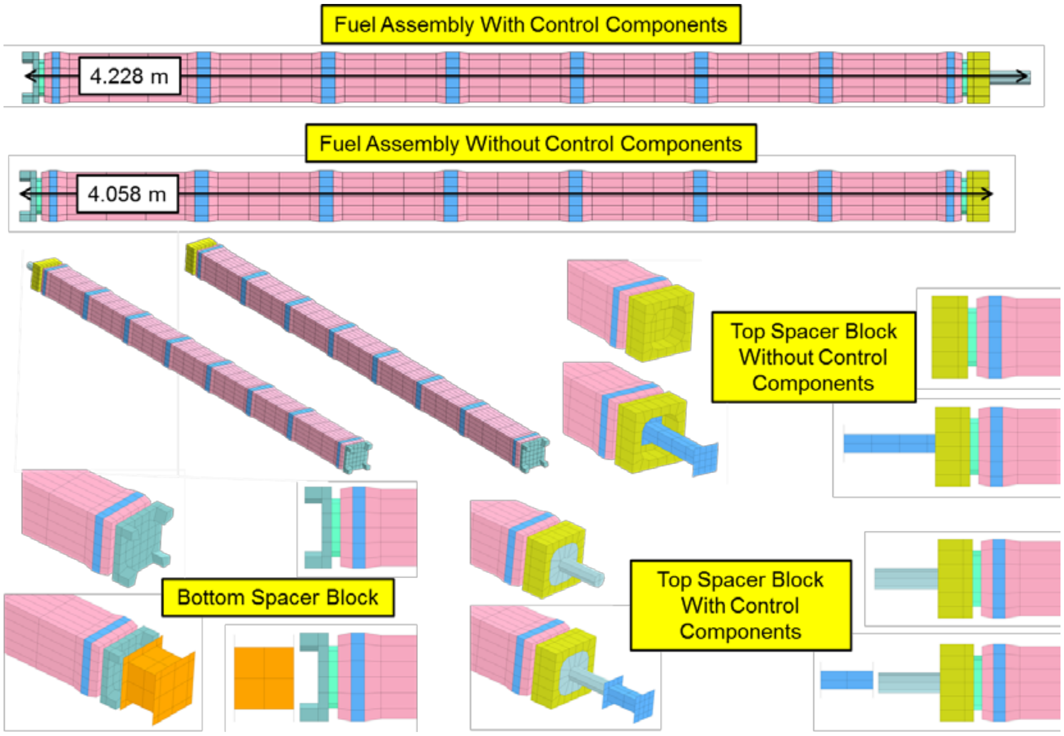

Figure 3: Fuel Assembly and Spacer Block Components of Cask Assembly Model.

Several cask assembly model configurations were investigated as part of a sensitivity study. These included two bounding model temperature distribution configurations (“hot” and “cold” [6]), two component-to-component spacing configurations (“nominal” and “large clearance”), and two fuel assembly configurations (“with” and “without” control components). The specific component temperatures used for each case are listed in Table 1 and the specific component-to-component clearances utilized are listed in Table 2.

Table 1: Cask Assembly Model Component Temperatures.

Case	Component Temp					
	Basket		Canister		Cask	
	(°F)	(°C)	(°F)	(°C)	(°F)	(°C)
Hot	560.0	293.3	342.0	172.2	194.6	90.3
Cold	127.7	53.2	68.9	20.5	44.0	6.7

Table 2: Cask Assembly Model Component-to-Component Gaps.

Dimension	GBC-32	Cask FEM Large Clearance	Cask FEM Nominal
Canister-to-Cask Clearance (Radial and Each End)	---	10 mm	5.0 mm
Basket-to-Canister Lateral Clearance (Radial)	---	10 mm	5.0 mm
Basket-to-Canister Axial Clearance (Each End)	---	25 mm	12.5 mm
Fuel-Assembly-to-Basket Lateral Clearance (All Sides)	---	6.0 mm	2.9 mm
Fuel-Assembly-to-Spacer-Block Axial Clearance (Each End)	---	20 mm	10 mm
Top Spacer Block Lateral Clearance to Basket (All Sides)	---	53.1 mm	50 mm
Bottom Spacer Block Lateral Clearance to Basket (All Sides)	---	8.1 mm	5 mm

LOAD CASES

A series of load cases, comprised of ten second duration six degree-of-freedom rail car acceleration time-histories extracted from longer measured (coal car) or simulation-generated (NUCARS®) rail car acceleration time-history datasets provided by TTCI, were produced [7]. Loads designated P1 (or Phase I) were extracted from several days' worth of measured acceleration time-history data for rail cars used to transport coal. Loads designated P3 (or Phase III) were extracted from acceleration time-history data from a series of NUCARS® simulations of the transport of UNF in a rail transportation cask. Because the P3 simulations utilized a cask model consistent with the generic cask assembly model described earlier, and a model of a rail car designed specifically for the purpose of transporting UNF, the P3 rail car data should be more representative of actual UNF rail transport environments than the P1 data. From each data set (P1 and P3) three excerpts (each consisting of time phased six degree-of-freedom acceleration time-histories) were selected to capture the peak shock event in each coordinate direction of "axial" along the track, "lateral", and "vertical", and three excerpts were selected to capture representative continuous vibrations excluding major shock loads for each of the three ("axial", "lateral", and "vertical") directions. Figure 4 illustrates this process for the P3 Shock Z (Vertical) load case. In the figure only the extracted translational acceleration time-histories are shown. For this load case three rotational acceleration time-histories (not shown in the figure) are also part of the load case definition. Note that the X, Y, Z direction designations associated with each load case refer to the TTCI loads coordinate system shown in Figure 5 and that the secondary designators of "Axial", "Lateral", and "Vertical" are used to avoid confusion in conversion of loads from the TTCI coordinate system to the coordinate system used in the FEM and shown in Figure 1. Table 3 summarizes pertinent information for each of the P1 and P3 load cases.

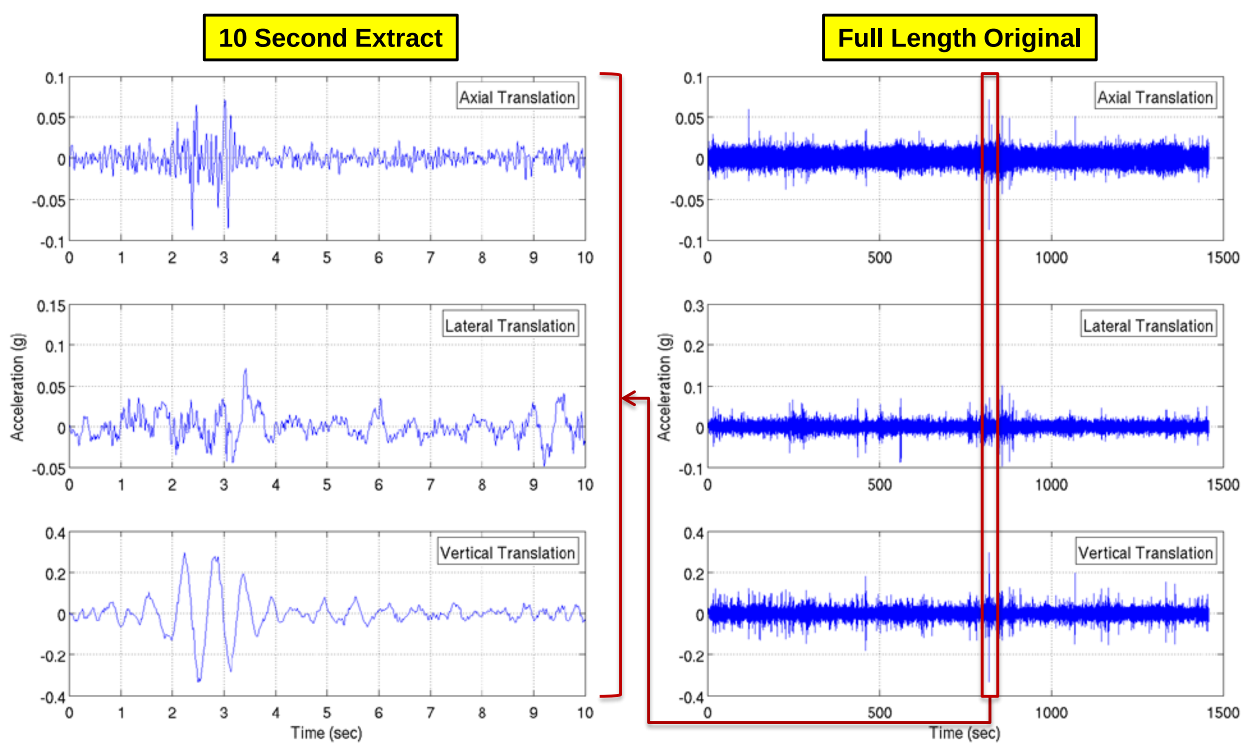

Figure 4: Translation Acceleration Time-History Excerpts for P3 Shock Z (Vertical) Load Case.

Table 3: P1 and P3 Load Case Peak Acceleration or g_{rms}.

Load Case	P1 Load Case	P3 Load Case
Shock X (Axial)	1.269 g	0.087 g
Shock Y (Lateral)	0.492 g	0.101 g
Shock Z (Vertical)	1.679 g	0.335 g
Vibration X (Axial)	0.0079 g_{rms}	0.00221 g_{rms}
Vibration Y (Lateral)	0.0105 g_{rms}	0.00318 g_{rms}
Vibration Z (Vertical)	0.0241 g_{rms}	0.00805 g_{rms}

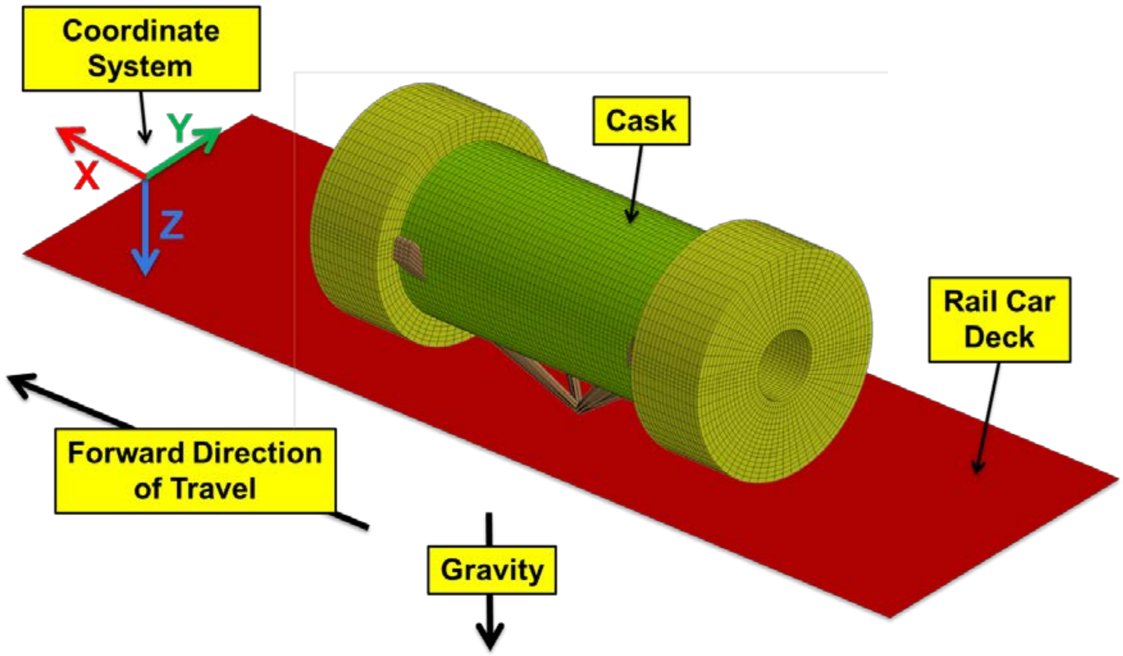

Figure 5: TTCI Rail Car Acceleration Coordinate System.

For comparison, NUREG/CR-0128 [10] defines shock and vibration environments for large shipping containers transported by truck [11]. These environments are defined for two packages, one with a total mass of 20,000 kg (44,000 lbm) and another with a total mass of 25,000 kg (56,000 lbm). Figure 6a shows a comparison of the shock response spectra (SRS) between the NUREG/CR-0128 shock environment and the P1 and P3 Shock Z (Vertical) load cases. The P1 Shock Z (Vertical) load case is very similar to the NUREG/CR-0128 shock environment, with the most pronounced difference being between 1 and 3 Hz in which the P1 load case shows an increased response magnitude over that of the NUREG/CR-0128 environment. Between 1 and 2 Hz the P3 Shock Z (Vertical) load case is more in-line with the NUREG/CR-0128 shock environment; however, at frequencies above 2 Hz the P3 load case produces a response well below that of the NUREG/CR-0128 shock environment (approximately 0.4 g versus 1.1 g, respectively). Figure 6b shows a comparison of the envelope of the power spectral density (PSD) curves for the NUREG/CR-0128 vibration environments and the PSD curves for the P1 and P3 Vibration Z (Vertical) load cases. Both the P1 and P3 vibration environments contain significantly less power than the NUREG/CR-0128 vibration environment across the frequency range from 1 to 500 Hz.

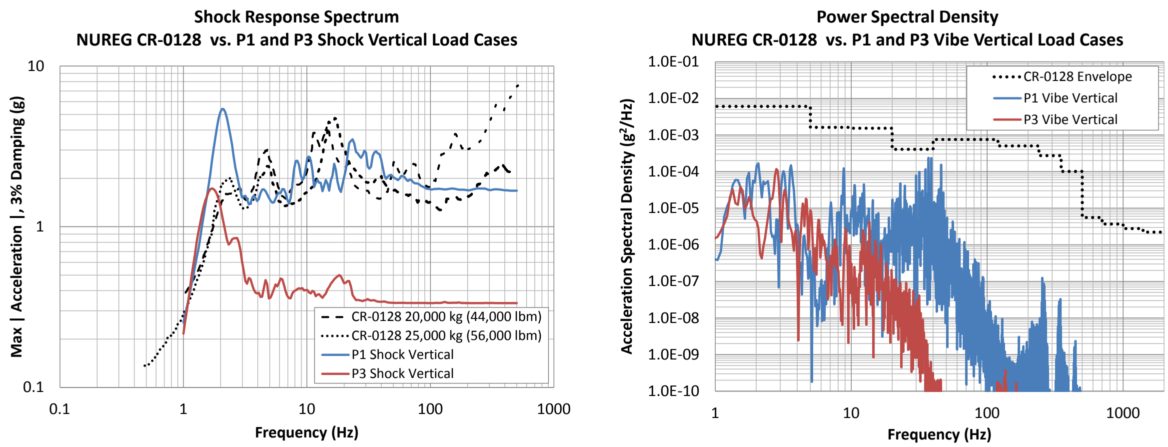

(a) Shock **(b) Vibration**

Figure 6: Comparison of the P1 and P3 Load Cases with the NUREG/CR-0128 Loads.

SIMULATION RESULTS AND DISCUSSION

Table 4 lists the simulations that were performed. The cask assembly model configuration that includes fuel assemblies with control components, "hot" component temperatures, and nominal component-to-component gap sizes constitutes the "nominal" cask configuration. For the nominal configuration, analyses utilizing each of the P1 and P3 load cases were performed. For the other "off-nominal" configurations investigated, analyses for only the P3 shock load cases were performed with the intent of assessing the sensitivity of response characteristics to off-nominal configuration changes. For each simulation, acceleration-velocity-displacement data in all six degrees-of-freedom were extracted at a series of locations on the basket and fuel assemblies. Figure 7 illustrates the specific output locations in more detail. Results from each analysis were assessed largely on examination and comparison of the average response of the basket at each basket cell center (see blue dots in Figure 7). Due to space limitations, only a brief overview of the main findings from these analyses is provided.

Table 4: Cask Assembly Model Simulation Matrix.

Load Case	Control Components	Temperature	Gap Size
P1 Shock X (Axial)	With	Hot	Nominal
P1 Shock Y (Lateral)	With	Hot	Nominal
P1 Shock Z (Vertical	With	Hot	Nominal
P1 Vibe X (Axial)	With	Hot	Nominal
P1 Vibe Y (Lateral)	With	Hot	Nominal
P1 Vibe Z (Vertical)	With	Hot	Nominal
P3 Shock Y (Lateral)	With	Hot	Nominal
P3 Shock Z (Vertical	With	Hot	Nominal
P3 Vibe X (Axial)	With	Hot	Nominal
P3 Vibe Y (Lateral)	With	Hot	Nominal
P3 Vibe Z (Vertical)	With	Hot	Nominal
P3 Shock Y (Lateral)	Without	Hot	Nominal
P3 Shock Z (Vertical)	Without	Hot	Nominal
P3 Shock Y (Lateral)	With	Cold	Nominal
P3 Shock Z (Vertical)	With	Cold	Nominal
P3 Shock Y (Lateral)	With	Hot	Large Clearance
P3 Shock Z (Vertical)	With	Hot	Large Clearance

Component and Location	Node ID Range
Rail Car – Node at Interface Between Cradle and Rail Car Deck	100
Basket Cell – Center	1XX's, Where XX = 01 to 31
Basket Cell – Corners at Fuel Assembly Ends, Mid-Point, and Quarter Points	10,0XX's, Where XX = 01 to 05
Basket Cell – Corners at Fuel Assembly Spacer Grid Mid-Points	10,0XX's, Where XX = 11 to 18
Basket Cell – Horiz. Walls at Fuel Assembly Ends, Mid-Point, and Quarter Points	20,0XX's, Where XX = 01 to 05
Basket Cell – Horiz. Walls at Fuel Assembly Spacer Grid Mid-Points	20,0XX's, Where XX = 11 to 18
Basket Cell – Vert. Walls at Fuel Assembly Ends, Mid-Point, and Quarter Points	30,0XX's, Where XX = 01 to 05
Basket Cell – Vert. Walls at Fuel Assembly Spacer Grid Mid-Points	30,0XX's, Where XX = 11 to 18
Top Spacer Block – Mid-point of Face On Fuel Assembly Side	40,0XX's, Where XX = 01 to 32
Bottom Spacer Block – Mid-point of Face On Fuel Assembly Side	50,0XX's, Where XX = 01 to 32
Fuel Assembly – Bottom Spacer Grid Mid-Points	1,000,000's

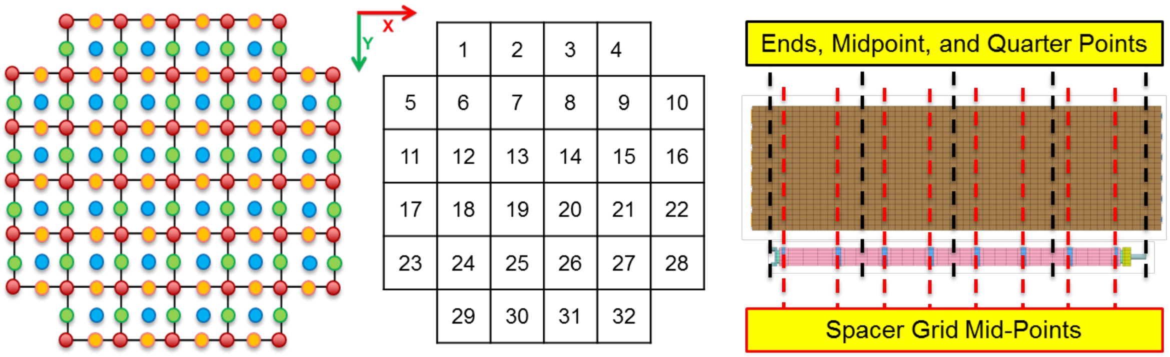

Figure 7: Cask Assembly Model Data Output Locations.

Nominal Configuration Results

For the cask assembly as realized in the cask assembly FEM, the shock and vibration loads derived from the P1 data provided by TTCI produced significant excitations at the fuel assembly level. In fact, in the axial and vertical shock cases, the rail car loads were severe enough to result in slip and/or vertical separation of the fuel assemblies in the basket and impact of the fuel assemblies against the top and bottom spacer blocks. Figure 8 illustrates the axial and lateral slip, and vertical separation plots for the cell 11 fuel assembly (see Figure 7 for basket cell numbering) for the P1 Shock X (Axial) and P1 Shock Z (Vertical) load cases. In the figure, the grey shading indicates the approximate location of the cell walls or top and bottom spacer blocks. Figure 8a indicates that in the P1 Shock X (Axial) load case a sudden slip axially and laterally of the cell 11 fuel assembly at about 2.5 seconds occurred, accompanied by a small vertical separation. The axial slip distance was approximately 20 mm in magnitude, which is equal to the total axial clearance between the fuel assembly and its spacer blocks, indicating that the fuel assembly slid axially in its cell and impacted its forward spacer block, and then rebounded, slid in the opposite direction, and impact its rear spacer block. (Note that because the method used to calculate the slip/separation is only approximate, the total axial slip calculated and indicated in Figure 8a is actually greater than the 20 mm of available slip distance.) Lateral slip of the cell 11 fuel assembly at 2.5 seconds had a peak-to-peak magnitude of approximately 3 mm which is less than the total lateral clearance between the fuel assembly and its cell walls of 5.8 mm. The vertical separation that accompanied the shock was limited to less than 1 mm. Similarly, for the P1 Shock Z (Vertical) load case (Figure 8b) the cell 11 fuel assembly separated from the basket and came close to or may have actually impacted the top wall of its cell. This vertical separation was accompanied by significant lateral and axial slippage.

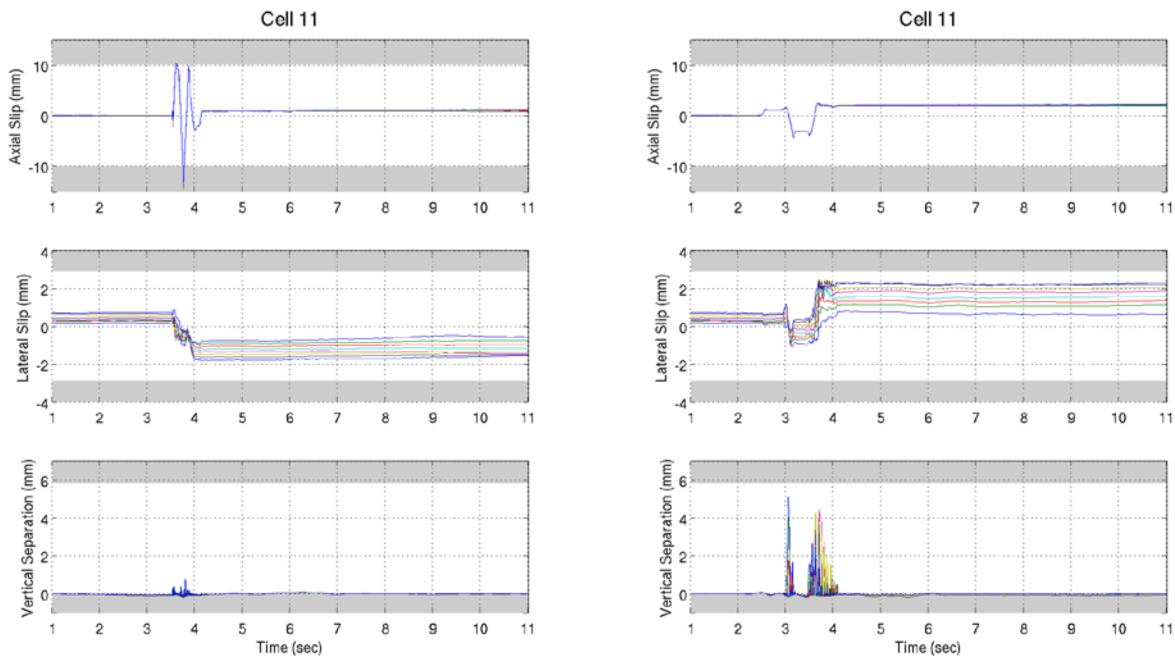

(a) P1 Shock X (Axial)

(b) P1 Shock Z (Vertical)

Figure 8: P1 Shock X (Axial) and P1 Shock Z (Vertical) Load Case Slip/Separation Plots.

P1 vibration loads were more benign than the P1 shock loads. Despite this they still tended to produce excitations at the fuel assemblies of significant magnitude in the frequency range of concern, namely between 10 and 60 Hz. Figure 9 shows the transfer functions and SRSs for the translational acceleration response degrees-of-freedom at all 32 basket cell locations for the P1 Vibration Z (Vertical) load case. The SRSs for the cell responses in the vertical translation degree-of-freedom (bottom plot in Figure 9b) indicate that the response of a fuel assembly or a fuel assembly component could be significant (between 1 and 2 g) at frequencies between 20 and 40 Hz if the assembly or component has a response mode between those frequencies (the fuel assemblies investigated in this study had response modes between 10 and 60 Hz). The transfer functions for the cell responses in the vertical translation degree-of-freedom (bottom plot in Figure 9a) indicate that the responses seen in the vertical direction in the SRS plots between 20 and 40 Hz are the result of amplification of the input excitations in the vertical direction at those frequencies, with amplification factors upwards of 6 observed for some of the cell locations.

The P3 shock and vibration loads derived from the NUCARS® simulations performed by TTCI produced basket cell excitations significantly reduced from those of the P1 shock load cases. Figure 10 illustrates this for the P1 and P3 Shock Z (Vertical) load cases. Comparison of the peak acceleration of about 4.5 g at 2 Hz in the SRSs for the cell responses in the vertical translation degree-of-freedom for the P1 load case (bottom plot in Figure 10a) against the peak acceleration of about 1.5 g at 2 Hz for the P3 load case (bottom plot in Figure 10b) clearly illustrates the difference. In addition, the peak response in the vertical direction in the P3 load case between 30 and 40 Hz was significantly reduced from the peak in the P1 load case (0.5 g versus 4.5 g, respectively). Despite the reduced severity of the P3 loads, the P3 shock loads were still severe enough to induce sliding and impact of the fuel assemblies in the basket in some cases.

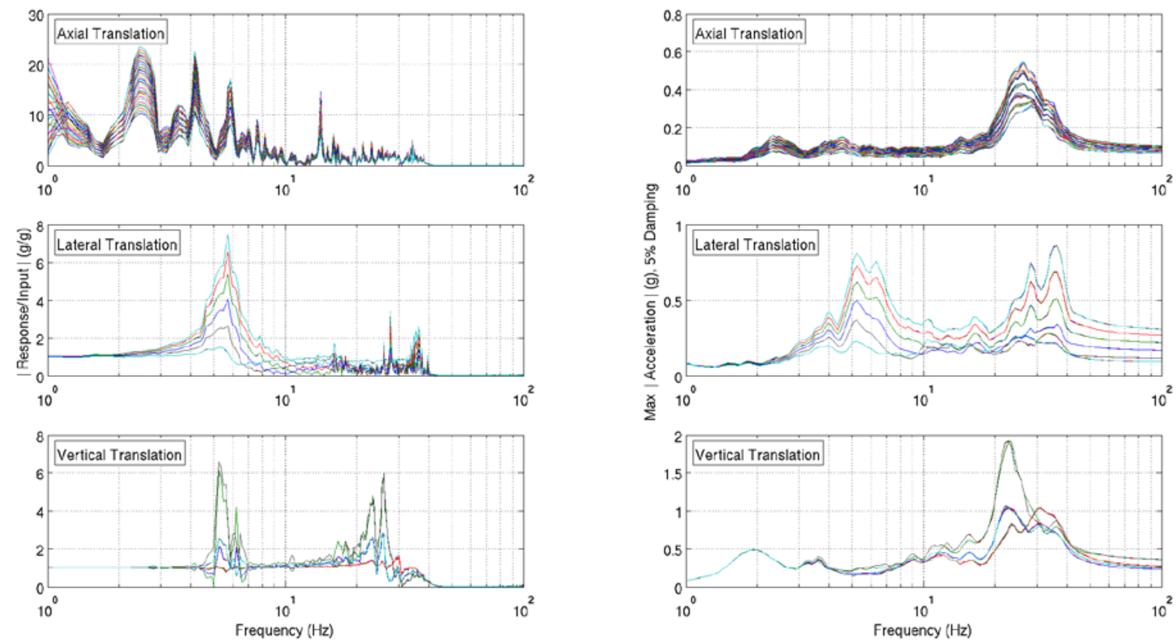

(a) Transfer Functions (b) SRSs

Figure 9: P1 Vibration Z (Vertical) Load Case Transfer Functions and SRSs.

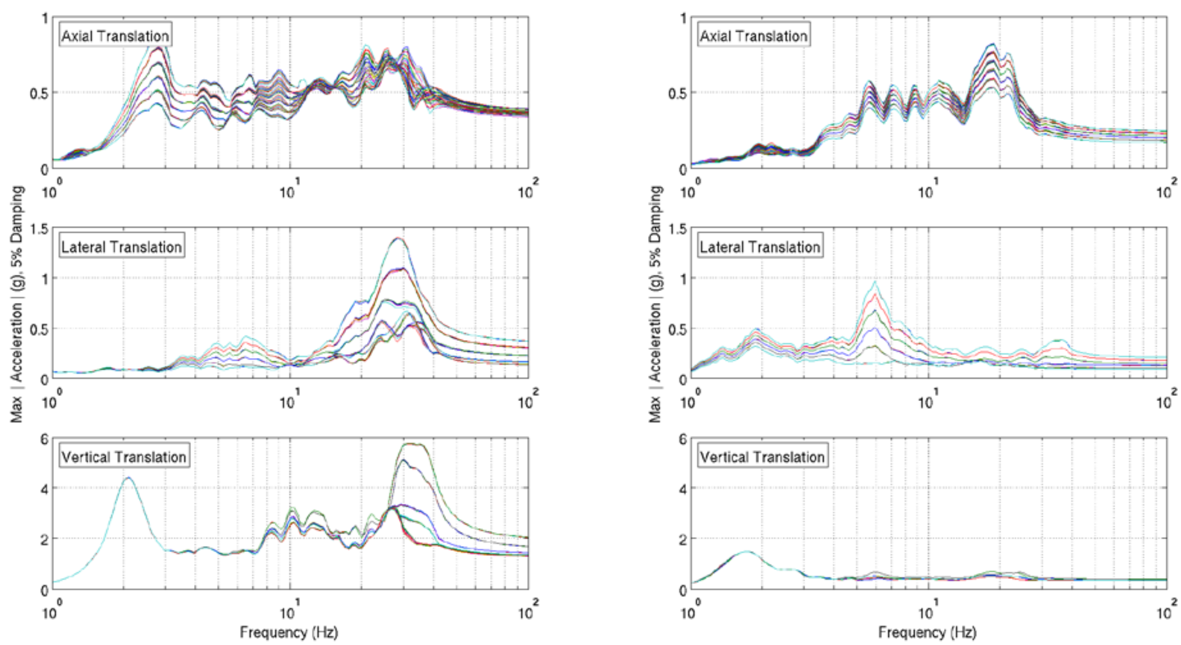

(a) P1 Shock Z (Vertical) SRSs (b) P3 Shock Z (Vertical) SRSs

Figure 10: P1 Shock Z (Vertical) and P3 Shock Z (Vertical) Load Case SRS Comparison.

The P3 vibration loads were generally more benign than even the P1 vibration loads, but still produced some level of excitations at the fuel assemblies in the frequency range between 10 and 60 Hz. Figure 11 shows the transfer functions and SRSs for the translational acceleration response degrees-of-freedom at all 32 basket cell locations for the P3 Vibration Z (Vertical) load case. Comparison of the SRSs for the cell responses in the vertical translation degree-of-freedom for the P3 load case (bottom plot in Figure 11b) with those for the P1 load case (bottom plot in Figure 9b) clearly highlights this difference. The peak vertical direction SRS acceleration for the P1 load case of nearly 2 g's is significantly higher than the peak vertical direction SRS acceleration for the P3 load case of only 0.3 g's. Figure 11b indicates that the response of a fuel assembly or a fuel assembly component could be about 0.2 g's at frequencies between 20 and 30 Hz if the assembly or component has response modes between those frequencies (again, the fuel assemblies investigated in this study had response modes between 10 and 60 Hz). The transfer function for the cell responses in the vertical translation degree-of-freedom (bottom plot in Figure 11a) indicate that the responses seen in the vertical direction in the SRS plots between 20 and 30 Hz are the result of amplification of the input excitations in the vertical direction at those frequencies, with amplification factors upwards of 14 observed for some of the cell locations.

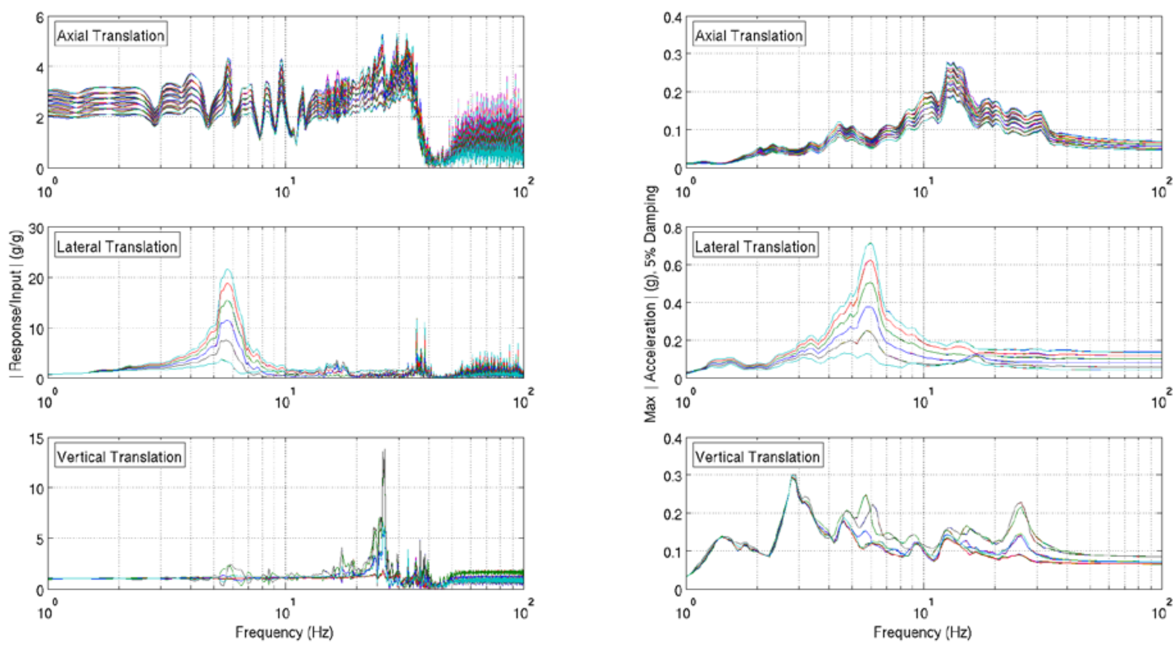

(a) Transfer Functions (b) SRSs

Figure 11: P3 Vibration Z (Vertical) Load Case Basket Cell Response Transfer Functions and SRSs.

Sensitivity Study Results

Results from the sensitivity analyses performed indicate that cask component temperature, for loads consistent with the P3 shock loads and for the range of temperatures expected, were relatively unimportant in determining the severity of the excitations at each fuel assembly; whereas the inclusion or exclusion of the control assembly components with each fuel assembly was found to be of moderate importance, and component-to-component gap size of significant importance. Figure 12 provides a comparison of SRS for the nominal configuration model and the large clearance configuration model for the P3 Shock Y (Lateral) load case. The figure illustrates that the peak response for the large clearance configuration was higher than that of the nominal configuration and in some instances significantly higher. In the lateral translation direction, the peak SRS magnitude at about 30 Hz for the large clearance case (3 g) was approximately 90% higher than in the nominal case (1.6 g). In the vertical translation direction the peak response for the large clearance case at 20 Hz (2.5 g) was higher by 150% than the peak for the nominal configuration at that frequency (1 g). Lateral sliding of the fuel assemblies within the basket cells and subsequent impact with the cell walls appeared to play an important role in the severity of the response in the large clearance case. Larger clearances appeared to facilitate the conversion of input energy at low frequencies (<10 Hz) into energy at higher frequencies, which are more in range with the response frequencies of interest for the fuel assemblies, namely 10 to 40 Hz.

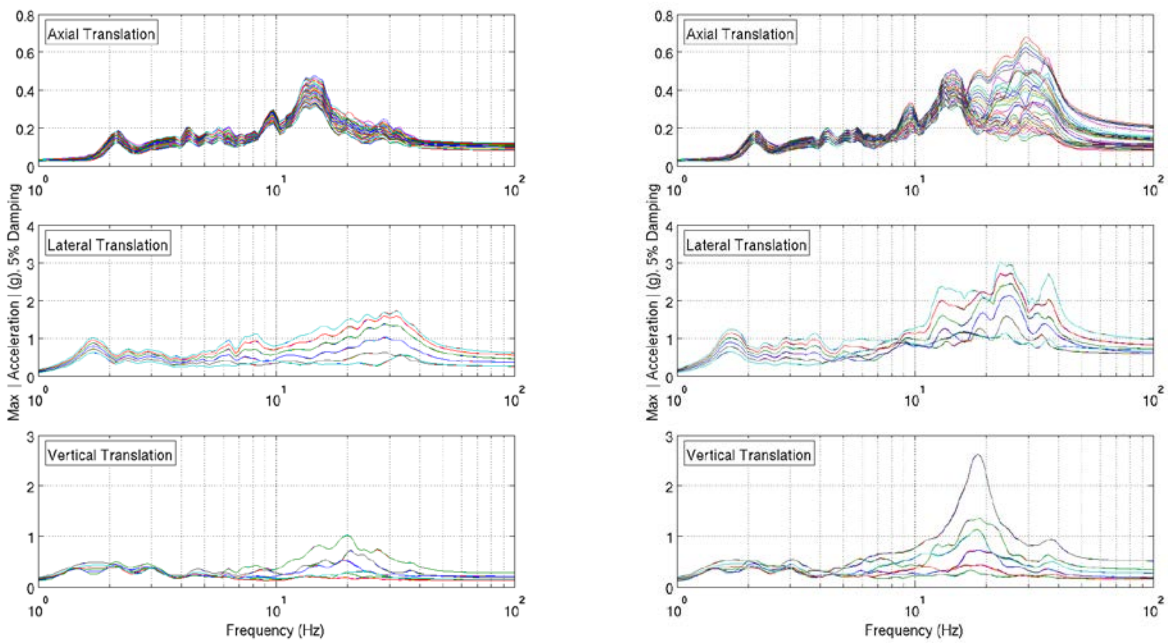

(a) Nominal Configuration - SRSs

(b) Large Clearance Configuration - SRSs

Figure 12: P3 Shock Y (Lateral) Load Case Nominal vs. Large Clearances Comparison.

Investigation of results from all of the analyses performed indicates that cell location within the basket was of critical importance in determining the characteristics and severity of the response. For example, cells located on the exterior edges of the basket displayed different response characteristics when excited in the vertical direction than cells located towards the interior of the basket. Consider the response of exterior cell 5 and interior cell 7 given in Figure 13 to the loading of the P1 Shock Z (Vertical) load case. It is clear from the figure that the magnitude of the response in the vertical direction at 30 Hz was significantly different between the exterior cell (cell 5) which had a greater magnitude of response at 30 Hz, than at the interior cell (cell 7) at the same frequency.

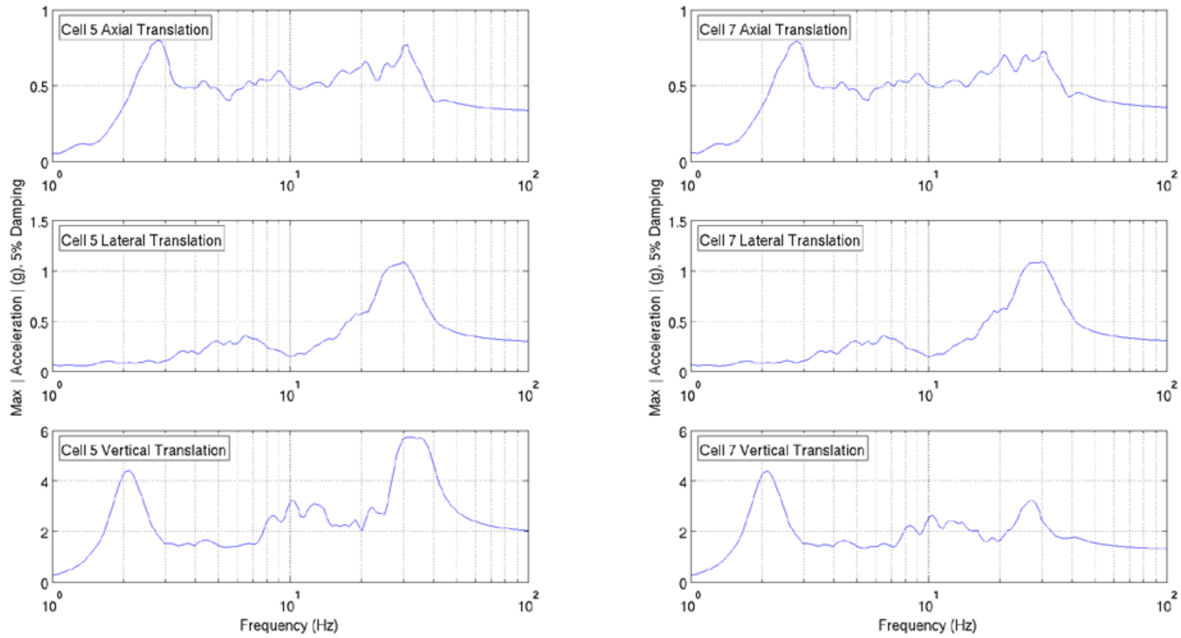

(a) Exterior Cell 5 – SRSs (b) Interior Cell 7 – SRSs

Figure 13: Comparison of Response in the P1 Shock Z (Vertical) Load Case Between an Interior and Exterior Cell.

OBSERVATIONS AND CONCLUSIONS

For the cask assembly as realized in the cask assembly FEM, the P3 shock and vibration loads derived from the NUCARS® simulations performed by TTCI (which are the most indicative of the loads that would be expected during rail transport of UNF on a purpose built rail car) in the case of the shock loads were severe enough in some instances to induce sliding of the fuel assemblies in the basket and impact of the fuel assemblies against either the basket cell walls or the top or bottom spacer blocks. In addition, the P3 vibration load cases produced loads at each basket cell location on the order of 0.2 g's in the frequency range at which a fuel assembly or its components would be expected to respond. While this acceleration is not large, this magnitude of loading at a loading frequency of 20 to 40 Hz over a transport lasting several days could be important when fatigue and fracture considerations are taken into account. Based on these observations, the following conclusions were drawn.

- Shock loads consistent with expected future rail transport of UNF on a purpose built rail car will likely be severe enough in some instances to cause sliding of the fuel assemblies within the cask basket assembly, and impact of the fuel assemblies against the basket walls or spacer blocks.

- Vibration loads consistent with expected future rail transport of UNF on a purpose built rail car are relatively small (~0.2 g's) in the frequency range of interest for UNF assemblies, but could potentially pose a risk when high cycle loading is considered.

Sensitivity studies performed as part of this work indicate that the size of clearances between components is important in determining the characteristics and severity of the loading environments produced at each cell location, with increasing clearance sizes generally resulting in more severe environments at each cell. In addition, cell location within the basket was also found to be important in this regard.

REFERENCES

1. J.T. Carter, A.J. Luptak, J. Gastelum, C. Stockman, and A. Miller, *Fuel Cycle Potential Waste Inventory for Disposition*, FCR&D-USED-2010-000031 Rev. 5, U.S. Department of Energy, Washington, D.C. (2012).
2. Blue Ribbon Commission on America's Nuclear Future, "Blue Ribbon Commission on America's Nuclear Future: Report to the Secretary of Energy", U.S. Department of Energy, Washington, D.C (2012).
3. U.S. Department of Energy, "Strategy for the Management and Disposal of Used Nuclear Fuel and High-Level Radioactive Waste", U.S. Department of Energy, Washington, D.C. (2013).
4. J.C. Wagner, "Computational Benchmark for Estimation of Reactivity Margin from Fission Products and Minor Actinides in PWR Burnup Credit", NUREG/CR-6747, ORNL/TM-2000/306, Oak Ridge National Laboratory, Oak Ridge, TN (2001).
5. K.J. Geelhood, "Used Nuclear Fuel Loading and Structural Performance Under Normal Conditions of Transport – Supporting Material Properties and Modeling Inputs", FCRD-UFD-2013-000123, U.S. Department of Energy, Washington, D.C (2013).
6. H.A. Adkins, "Used Nuclear Fuel Loading and Structural Performance Under Normal Conditions of Transport – Final Data, Material Property, and M&S Input Information", FCRD-TIO-2013-000255, U.S. Department of Energy, Washington D.C. (2013).
7. C. Urban, N. Wilson, and A. Keylin, "NUCARS® Modeling Support for DOE Used Nuclear Fuel Disposition, Task 2: NUCARS® Simulation of Representative Railcar", ORNL-13-002, Transportation Technology Center, Inc., Pueblo, C.O. (2013).
8. LS-DYNA (Version mpp d R6.1.1 Revision 79036 [Software]), Livermore Software Technology Corporation (LSTC), Livermore, C.A. (2013).
9. LSTC, LS-DYNA Keywords User's Manual Volume I and Volume II, Version 971 R6.1.0. Livermore Software Technology Corporation (LSTC), Livermore, C.A. (2012).
10. C.F. Magnuson, "Shock and Vibration Environments For A Large Shipping Container During Truck Transport (Part II)", NUREG/CR-0128, SAND78-0337, Sandia National Laboratories, Albuquerque, N.M. (1980).
11. U.S. Nuclear Regulatory Commission, "Standard Review Plan for Transportation Packages for Radioactive Material", NUREG-1609, Spent Fuel Project Office, Office of Nuclear Material Safety and Safeguards, U.S. Nuclear Regulatory Commission, Washington, D.C. (1999).